NONIMAGING FRESNEL LENS CONCENTRATOR—THE PROTOTYPE

Ralf Leutz[*†], **Akio Suzuki**[**], **Atsushi Akisawa**[*] **and Takao Kashiwagi**[*]

[*]Tokyo University of Agriculture and Technology,
Department of Mechanical Systems Engineering
2-24-16 Naka–cho, Koganei–shi, Tokyo 184-8588, Japan
[†] email ralf@star.cad.mech.tuat.ac.jp, phone/fax +81-42-388-7076

[**]UNESCO,
Bouvin 3.26 SC/EST, 1, rue Miollis, 75732 Paris Cedex 15

Abstract – Design, manufacturing, and preliminary tests of the prototype of a novel nonimaging Fresnel lens solar collector of medium concentration are presented. The collector is evaluated due to the optical concentration ratio of its lens, and the flux density on the absorber. The latter is discussed in detail in its suitability for photovoltaic applications. Costs of concentrating photovoltaic systems, as opposed to flat plate systems, are analysed. None of the systems is found to have a clear cost advantage over its competitors.

Fresnel Lenses for Solar Concentration

Fresnel lenses can be suitable solar concentrators. Lenses manufactured from Polymethylmetacrylate (PMMA) are characterized by high efficiency due to the high transmissivity of the material. Acrylic resin is lightweight, and resistant to ultraviolet rays. The Fresnel lens can be moulded, or extruded, which offers potential cost advantages over comparable solar concentrators operating on the reflective principle, notably the Compound Parabolic Concentrator (CPC).

A drawback of Fresnel lenses used to be the sensitivity of their optical performance on changes of the angle of the incident light. Conventional imaging Fresnel lenses require two–axis tracking of the sun. Commercially introduced has been the lens by O'Neill (1978), which is somewhat forgiving to problems of imaging (such as the size of the solar disc), thus showing the limits of imaging designs. This drawback was overcome with the introduction of nonimaging optics to the design of Fresnel lenses, marked by the works of Collares–Pereira (1979), Kritchman *et al.* (1979), and Lorenzo and Luque (1981). An optimum nonimaging Fresnel lens design has been presented by the authors (Leutz *et al.*, 1999a). The optimum shape of the 2D lens designed is found numerically incorporating three–dimensional refraction, minimum deviation prisms, and the edge ray principle of Welford and Winston (1989). Not photographic imaging counts, but the homogeneous illumination of a receiver. Two pairs if acceptance half angles are defined, θ in the cross–sectional plane, and ψ perpendicularly to it. They are spanning a part of the hemisphere, thus opening a window through which the concentrator 'sees' the sun. Fresnel lenses of nonimaging design are usually (but not necessarily) of convex shape, while their imaging counterparts are most often flat.

The novel nonimaging Fresnel lens can be designed as stationary solar collector of low concentration ratio (right side in Fig. 1). Medium and high concentration ratios call for one–axis (passive) tracking, and full tracking, respectively. A prototype of an optimum nonimaging Fresnel lens with a geometrical concentration ratio of 19.1 ('medium') has been designed, manufactured, and tested (left side in Fig. 1). Its acceptance half angles are $\theta = \pm 2°$, and $\psi = \pm 12°$, in the cross–sectional, and perpendicular planes, respectively. Note that Fig. 1 shows a cross–sectional view of the lenses, where θ is measured in the plane of the paper, while ψ cannot be seen as it must be drawn in the plane perpendicular to the paper surface.

The lens is intended for both photovoltaic, and solar thermal applications. Differences and common aspects in

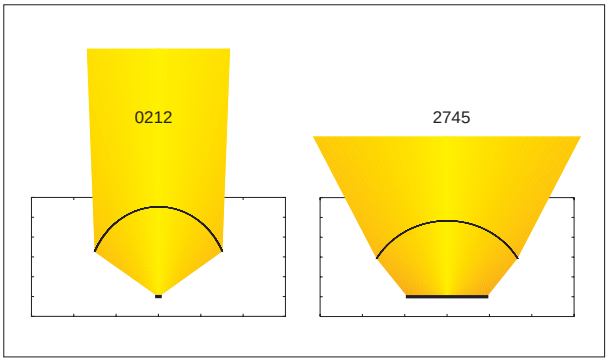

Figure 1: Schematic comparison of tracking and stationary type nonimaging Fresnel lenses. Acceptance half angles 2° in the cross–section (plane of paper), 12° in the perpendicular plane for a lens with concentration ratio $C = 19.1$. Values for the stationary concentrator 27°, 45°, $C = 1.7$. Projection into the cross–sectional plane.

the utilization of the nonimaging Fresnel lens for pv and solar thermal systems have been discussed earlier (Leutz *et al.*, 1999b). The distinction of mirrors for solar thermal use on the one side, and lenses for photovoltaics on the other has little technical justification. The separation seems rather metaphorical, and evolved historically.

Prototype Design

The design of the nonimaging Fresnel lens shown in Fig. 6 has been described in detail in Leutz *et al.* (1999a). Based on the priciples of edge rays, and minimum deviation prisms, under the condition of a smooth outer surface, the optimum shaped Fresnel lens has been found in a numerical simulation. The design of the line–focusing lens is based on the definition of two pairs of acceptance half angles: θ in the cross–sectional plane (the plane of the fixtures in Fig. 6, and ψ in the plane perpendicular to it.

Contrary to common imaging designs, the prisms in our lens are not equaldistant when assembled horizontally. In the shaped version of the lens, each prism covers a angular segment similar to those formed by the spokes of a wheel, but without its circular shape. The lens to be the first prototype was chosen to be of acceptance half angles $\theta = 2°$ and $\psi = 12°$. The lens was truncated at half height based on previous findings that found the performance of a truncated lens only slightly inferior to the one of a full lens (Leutz *et al.*, 1999a).

The lens is prepared for manufacturing by simulating its width according to the maximum dimensions given. The absorber width is found accordingly. The number of prisms and their coordinates in the shaped lens are calculated under the restrictions of given maximum groove depth. It is helpful to be able to have an additional degree of freedom in the simulation, which is the possibility to backstep, i.e. starting a new prism from any given point on the front face of the previous one, thus avoiding the thickness of the lens to be zero at the grooves. The effects of the 1.0 mm acrylic sheet for refraction (refraction at a plane parallel plate) are dismissed as insignificant on the grounds of being very small.

In a first step (see Fig. 2(a)), the prisms are moved into a horizontal position, and rotated until their front faces form a smooth flat line. The second step deals with the changes necessary due to the centerline requirement for pressing. A prism is chosen to serve as reference for setting the position of the centerline. Prisms from the reference prism towards the center of the lens are increased in size in order to have their back faces (which are almost parallel to their front faces, making the prism very 'thin') cross the centerline at a point where the elevation distances between groove and tip are equal. Outward prisms are decreased in size until the

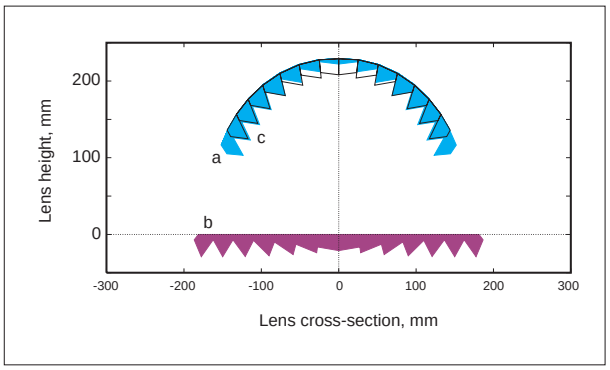

Figure 2: Preparations for manufacturing the Fresnel lens prototype. The prisms of an optimum shaped lens (a) are moved and rotated to form a flat sheet (b). Prism tips and grooves are arranged equaldistant to a centerline for ease of moulding. Resized prisms are brought back into shape (c).

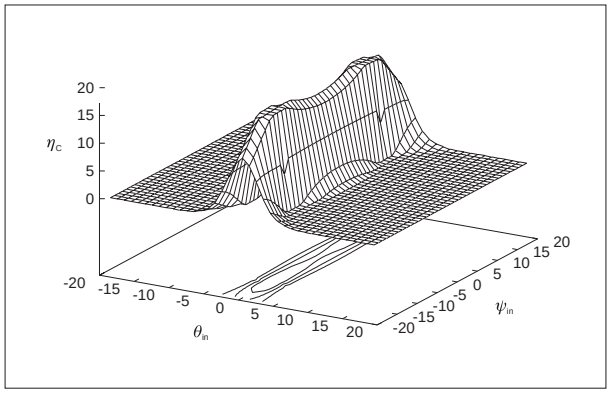

Figure 3: Optical concentration ratio for the lens of acceptance half angle pairs $\theta = \pm 2°$, and $\psi = \pm 12°$. Ray tracing, rays incident at θ_{in} represent the cross–sectional fraction of the hemisphere over the concentrator, ψ_{in} the perpendicular part.

same condition is fulfilled. The centerline condition facilitates ease of pressing the lens shape into a PMMA sheet. The coordinates of these prisms (Fig. 2(b)) are given to the manufacturer.

In a third step (Fig. 2(c)), the resized prisms of the flat lens are rearranged into the arched shape for two purposes. Small differences are observed to the original shape due to the resized prisms. The new lens shape must be known to first, produce a frame into which the bent lens is to be fixed and, second, to evaluate the newly shaped lens by ray tracing.

Prototype Manufacturing

Contrary to the common process of making flat Fresnel lenses, the manufacturing of shaped lenses is rarely undertaken. The tips of the prisms constituting the lens are creating an undercut, thus moulding of the shaped lens can only be achieved when a mould with collapsable core is used. Extruding of the lens runs into equal difficulties due to its rolling stage. Considering limited funding, it was decided to produce the shaped lens as flat sheet to be bent into its optimum shape. Sheet lenses (examples being imaging lenses used in overhead projection, or copy machines) are usually pressed.

In a simulation the prisms of the shaped Fresnel lens are rotated and moved until they form a flat sheet lens. Manufacturing makes it necessary to increase or decrease the size of each prism in order to obtain a centerline common to all prisms. This line is defined by choosing the size of a suitable prism as normal. The vertical distance between prism tips and grooves should not exceed 0.5 mm, in order to allow for pressing the lens contours into a PMMA–sheet of 1.0 mm thickness. A prototype of the 0212–lens was manufactured by Nihon Fresnel, Ltd., of Tokyo, Japan. Sheets of $400.0 \times 400.0 \times 1.0$ mm become lenses in the following steps:

A negative of the lens contours is turned on a numerically controlled lathe using a diamond cutter. Although only the surface of the prism face has to be highly finished, the unused prism back receives the same accurate treatment. The machine is designed for accuracies of 1/1000 mm for lengths, and 1/100° for angles.

A single PMMA–sheet is heated for about 3.5 min at 280℃ applying a pressure of 625 kg/m^2 (6.13 kPa). The hot sheet is pressed onto the negative form for another 3 min at similar conditions of pressure and temperature. One negative can be used to produce around 2,000 lenses with sufficient accuracy, if hard spots in the acrylic sheet are removed beforehand.

The process described can only be used if the outer surface of the lens is smooth. A second grooved surface cannot be obtained with satisfactory accuracy with this production method, as both sides would have to be congruent. Furthermore, the prisms have to be small, or pressing is not possible. This leads to a high number of prisms, and high accuracy for a large number of prisms is required in the carving of the metal negative. Also, the size of the lens is limited. Finally, the pressing process is a batch process, output is smaller than using extrusion.

Fresnel Lens Performance

The prototype lens is bent into shape by fixing the flat sheet into a frame that serves as test rig. Note that the shape of the lens is not circular, but results from the definition of both acceptance half angles. A comparison of shapes for the tracking prototype 0212–lens, and a stationary lens designed with acceptance half angles 27° and 45° in its cross–section, and perpendicular to it, is given in Fig. 1. The width of the flat lens is the fixed parameter in the schematic. The qualitative relations of absorber width, acceptance half angles (represented by the cross–sectional design angle θ), and geometrical concentration ratio C are obvious.

$$C = \frac{1}{\sin\theta} \tag{1}$$

Both lenses in Fig. 1 are truncated at half height above the absorber. The performance of a solar concentrator is simulated with the ray–tracing procedure. Incident rays are generated spanning the hemisphere. Their paths through the lens, and towards the absorber are followed. Depending on their angle of incidence, some ray paths will be blocked by an adjacent prism's tip. In other cases, the prism tip may not be fully filled with light, as the groove of the previous prism leads to reflection on the prism's back. Rays missing the absorber due to blocking losses L_b or unused tip losses L_u, and transmissivity τ accounting for first order reflection losses are counted as total losses. The optical performance of the lens is measured in terms of an optical efficiency, stating the ratio of solar rays hitting the absorber to the radiation incident on the outside of the lens I_{in}. Expressed in absolute terms, the optical efficiency η is

$$\eta = I_{in} - (L_b + L_u + \tau) \tag{2}$$

The optical efficiency of the lens represents only one of the characteristics of the concentrator. Multiplying the geometrical concentration ratio with the optical efficiency of the lens makes the concentrator comparable to other concentrators. The resulting value, the optical concentration ratio η_C describes the ratio of radiation intensity without concentrator by radiation intensity with concentrator.

$$\eta_C = C\,\eta \tag{3}$$

The optical concentration ratio of the 0212–lens has been plotted over rays incident in both the cross–sectional plane θ_{in}, and the perpendicular plane ψ_{in} in Fig. 3. The plateau and sharply dropping sides are characteristic of nonimaging concentrators. Average values for the performance of the lens within the design angles can be calculated. Actual values differ from the equations given above since the geometrical concentration ratio C is found as the ratio of the width filled by rays entering the outer lens surface by the width of the absorber. The width of the first aperture is corrected by the cosine–losses (the surface is corrected for its shape to make it comparable with other concentrators where the first aperture is usually flat), and the optical concentration ratio is in fact a projective optical concentration ratio, calculated not with the geometrical concentration ratio C of Eqn. 1 but with a slightly different projective concentration ratio.

Furthermore, the mathematical expression for the geometrical concentration ratio C is true only for the ideal 2D concentrator. Eqn. 1 is at best an approximation for the nonimaging Fresnel lens, which in paractice is nonideal. The geometrical concentration ratio of an ideal concentrator with a cross–sectional acceptance half

angle of 2° is $C = 1/\sin(2) = 28.7$. This obscures the fact that the perpendicular acceptance half angle plays an important role in restricting the concentration ratio of the lens. A more detailed discussion of the variety of concentration ratios is given in Leutz *et al.* (1999a).

Absorber Flux

The width d of the absorber of the nonimaging Fresnel lens is correlated with the lens height h and the cross–sectional acceptance half angle θ

$$h = \frac{d}{\tan\theta} \tag{4}$$

This is different from imaging lens design, where the focal point is found as intersection of the conjugate with the refracted rays, depending on the power of the lens. If a finite size absorber is to be placed behind an imaging lens, its position may be found by applying the concept of a 'circle of least confusion', which describes a plane defined by the intersection of the refracted rays of the longest design wavelength from the right side of the lens, and the refracted ray of the shortest design wavelength from the left side of the lens (and vice versa). See Boise Pearson and Watson (1998) for a discussion.

Even in the nonimaging 2D–lens, the absorber width is greater than the cross–section of the area filled by light incident at a combination of rays θ_{in}/ψ_{in}. The size of the fraction filled, and its location on the absorber must be known in order to evaluate the suitability of the lens for photovoltaic applications where homogeneous illumination of the absorber in terms of both flux density, and color spectrum is essential for the performance of the system. Inhomogeneous illumination of the absorber due to the way the different colors of the solar spectrum are refracted is presented in Leutz *et al.* (1999b).

The flux density on the absorber can be calculated by tracing incident edge rays from the lens to the absorber. Once the geometrical losses (see Eqn. 2) are discounted, an effective width w of the lens is found. Transmission losses τ accounting for first order reflections are deducted. The edge (maximum) rays for any combination of incidence are traced, and their intersections with the absorber plane are found in a cross–sectional projection, resulting in a part of the absorber plane δd being illuminated. Depending on the distance of the prism from the absorber, a factor s describing the spread of the refracted beam is calculated. The prism's height over the absorber plane defines the cosine losses of the beam when hitting the absorber at an angle β other than normal. The procedure is repeated for each prism i on both sides of the 2D–lens. The two sides are not symmetric for any combination of incidence other than normal incidence. The resulting values are cumulated according to their location on the absorber. Thus, the flux density on any part of the absorber plane $\delta\xi$ is found as

$$\delta\xi\,(\theta_{in}, \psi_{in}) = \sum_{-i}^{i} w\ \tau\ s\ \cos\beta \tag{5}$$

This flux density ξ is summed up into one cross–sectional plane for any combination of incidence, implying that no end effects of the 2D–lens are considered. The flux density is for the second (exit) aperture of the optical system, what the optical concentration ratio is for the first aperture: it describes the effect of the concentrator.

Figure 4 depicts flux densitied for various combinations of incidence, for a lens with the design acceptance half angles $\theta = 2°$ in the cross–sectional plane, and $\psi = 12°$ in the perpendicular plane. The absorber extends from -7.9 to 7.9 units. The influence of the perpendicular incidence angle ψ can clearly be seen. As expected, the flux density ξ is most clearly defined for the cases of normal incidence, and incidence at design angles. Other combinations of incidence yield flux distributions where the steep flanks characteristic to nonimaging systems are less clearly visible.

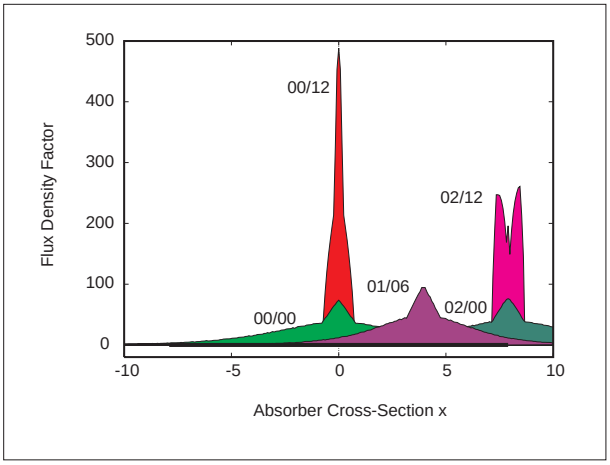

Figure 4: Cumulative flux density on the absorber of a lens of acceptance half angle pairs $\theta = \pm 2°$, and $\psi = \pm 12°$. Combinations of incident rays; yellow light only. Cross–sectional view of long lens.

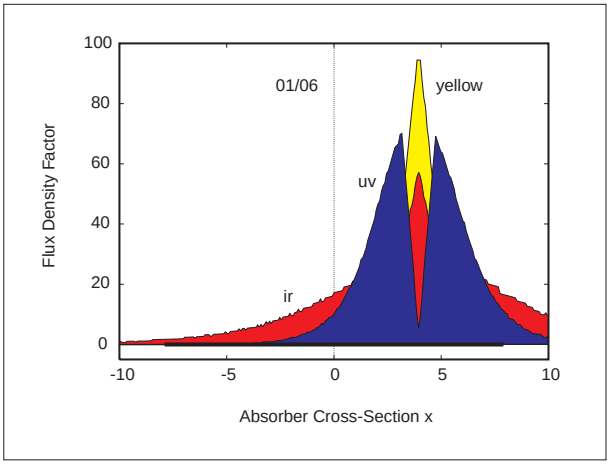

Figure 5: Cumulative flux density on the absorber of a lens of acceptance half angle pairs $\theta = \pm 2°$, and $\psi = \pm 12°$. Incidence at $\theta_{in} = 1°$, and $\psi_{in} = 6°$. For wavelength dependent refractive indices over the range of the solar spectrum. Graphs do not represent the respective fraction of wavelength energies in solar irradiance. Cross–sectional view.

The graphs of Fig. 4 are somewhat misleading as they are drawn only for incidence of yellow light, with a corresponding refractive index of 1.49 for polymethylmetacrylate. Sunlight covers a wide spectrum, and wavelength dependent refractive indices are in the range from 1.515 for near ultraviolet light (350 nm), and 1.48 for light in the near infrared (1,500 nm). Using these refractive indices, the illumination of the absorber appears more complete, while colors still mix considerably. An example for the same 02/12–lens, and incidence at $\theta_{in} = 1°$ and $\psi_{in} = 6°$ is given in Fig. 5.

The advantages of the nonimgaing design are its reduced tracking requirements, and color mixing, but a price has to be paid: illumination remains incomplete. A secondary concentrator may be called for, at least for photovoltaic applications. Solar thermal systems are less affected in their performance by 'hot spots', and may operate without secondary concentrator. The performance of actual system will decide these uncertainties.

Cost Considerations

Estimating the cost of a new solar concentrator is, as with most products, a difficult undertaking. Not only that little is known about the actual performance and application of the novel nonimaging Fresnel lens, but cost data for comparable systems are first, difficult to obtain, and second, due to the systems' limited dissemination in an often subsidized (national) market, are unreliable. The technology of Fresnel lenses for solar applications is mature, but the markets are not.

A condensed cost study for solar concentrators, including Fresnel lenses for photovoltaics has been published by Boes and Luque (1992). The following considerations (Tab. 1) are based on their meta analysis, data are backed up by traceable numbers circulated on the Solar–Concentrator (current) discussion group on the internet.

The idea behind solar concentration for photovoltaics is, of course, to save costly area of semiconductor cells. While concentrator cells are more expensive than conventional ones, and cost is added for the concentrator, and a tracking mechanism, the specific turn–key cost of a project tends to decrease when concentration technology is used. There are three factors related to the considerations in Tab. 1 that have to be pointed out.

- Availability, and technical maturity of concentrator technologies: full tracking requires high accuracies, if a

concentration of 1000X is to be employed. The reliability of both the optical system and potential trackers may be uncertain for some applications, and only suitable for systems in areas, where infrastructure allows constant supervision.

- Radiation: concentrators can collect only direct solar radiation. While they are tracking the sun, which results in a potentially higher yield due to reduced cosine losses, concentrating systems may be unsuitable for tropical climates where the diffuse fraction of sunlight is larger. The values given for Guam, and Barstow, CA, in the notes to Tab. 1 illustrate this.
- Flat plate developments: emerging manufacturing technologies, and new materials for flat plate photovoltaic systems are reducing the cost of these considerably. Crystalline silicone cells are accounting for roughly the same cost as concentrator technology. It remains to be seen whether the potential for cost reductions is greater for cells, or for concentrating technology.

The nonimaging Fresnel lens is an emerging concentrator technology, although a comparable system (O'Neill and McDanal, 1994) is in its market penetration phase, with apparently good results, and great expectations in possible cost reductions.

Conclusions

The comparison of cost trends in photovoltaic technologies as presented here results in none of the paths to be clearly favoured. Markets and technologies are not mature enough to allow for definite recommendations. Potentials for future cost reductions can hardly be estimated. It can be stated, however, that concentrators are best suited for possibly grid connected systems in climates with a high fraction of direct radiation.

This paper discussed the design, manufacturing, and evaluation of a novel nonimaging Fresnel lens concentrator for solar energy collection. The application of nonimaging principles allows for the design of even stationary solar collectors using Fresnel lenses. The prototype of a lens with medium concentration ratio is presented, and some of its properties are discussed. The optical concentration ratio of the lens, and the flux density on the absorber are described.

While the lens is a lightweight, cost–effective, and efficient concentrator, substantially lowering the requirements for tracking for line–focusing solar collectors, the absorber is not fully, or not homogeneously illuminated. The actual performance of a system using the lens will have to be evaluated after an absorber test rig has been built and field tests are carried out.

References

E. C. Boes, A. Luque (1992) Photovoltaic Concentrator Technology; in: T. B. Johansson, H. Kelly, A. K. N. Reddy, R. H. Williams (eds.): Renewable Energy, Sources for Fuel and Electricity, Washington, D.C.

J. Boise Pearson, M. D. Watson (1998) Analytical Study of the Relationship Between Absorber Cavity and Solar Fresnel Concentrator; *Proceedings of the International Solar Energy Conference; ASME*, 351-356, 14-17 June, Albuquerque, NM

D. E. Carlson, S. Wagner (1992) Amorphous Silicone Photovoltaic Systems; in: T. B. Johansson, H. Kelly, A. K. N. Reddy, R. H. Williams (eds.): Renewable Energy, Sources for Fuel and Electricity, Washington, D.C.

M. Collares–Pereira (1979) High Temperature Solar Collector with Optimal Concentration: Non–Focusing Fresnel Lens with Secondary Concentrator; *Solar Energy* **23**, 409-420

E. M. Kritchman, A. A. Friesem, G. Yekutieli (1979) Efficient Fresnel Lens for Solar Concentration; *Solar Energy* **22**, 119-123

R. Leutz, A. Suzuki, A. Akisawa, T. Kashiwagi (1999a) Design of a Nonimaging Fresnel Lens for Solar Concentrators; *Solar Energy*, **65**, 6, 379-388

R. Leutz, A. Suzuki, A. Akisawa, T. Kashiwagi (1999b) Nonimaging Fresnel Lens Concentrators for Photovoltaic Applications; *Proceedings of the ISES Solar World Congress*, 4-9 July, Jerusalem

E. Lorenzo, A. Luque (1981) Fresnel Lens Analysis for Solar Energy Applications; *Applied Optics* **20**, 17, 2941-2945

M. J. O'Neill (1978) Solar Concentrator and Energy Collection System; United States Patent 4069812

M. J. O'Neill, A. J. McDanal (1994) Fourth–Generation Concentrator System: From the Lab to the Factory to the Field; *1994 IEEE First World Conference on Photovoltaic Energy Conversion, Conference Record of the Twenty Fourth IEEE Photovoltaic Specialists Conference*, Vol. 1, 816-819, 5-9 December, Waikoloa, Hawaii, United States of America

NREL (National Renewable Energy Laboratory) (no year) Resource Assessment Program; available at *http://rredc.nrel.gov/solar/old_data/nsrdb/redbook/atlas/*

A. Rabl (1976) Optical and Thermal Properties of Compound Parabolic Concentrators; *Solar Energy* **18**, 497-511

Solar–Concentrator discussion group on the internet; archives at *http://www.scruz.net/~cichlid/solar-concentrator-archive*

W. T. Welford, R. Winston (1989) High Collection Nonimaging Optics, San Diego

K. Zweibel, A. M. Barnett (1992) Polycrystalline Thin–Film Photovoltaics; in: T. B. Johansson, H. Kelly, A. K. N. Reddy, R. H. Williams (eds.): Renewable Energy, Sources for Fuel and Electricity, Washington, D.C.

Table 1: Cost estimations for photovoltaic systems of various concentration (suns[1]). In US$/m^2 of collector, except where noted. Source: Boes and Luque (1992), Zweibel and Barnett (1992); authors' calculations.

Concentration (suns)[2]	1X	20X	1000X
Fresnel lens concentrator	–	30	30
Photovoltaic cells	320	25	75
Module[3]	**400**	**140**	**200**
Array structures/tracking	80	200	300
Power conditioning	20	40	40
Land	4	4	4
Direct cost	**524**	**384**	**544**
Indirect cost[4]	175	128	181
Total cost	**699**	**512**	**725**
Optical efficiency η_{lens}	0.95	0.75	0.90
Cell and power conversion efficiency η_{cell}[5]	0.15	0.20	0.25
Radiation utilizability $\eta_{radiation}$[6]	1.0	0.8	0.8
Output[6], W_p	143	120	180
Turn–key cost, \$/W$_p$	**4.90**	**4.30**	**4.00**

[1]Ideal geometrical concentration, calculated with irradiance of 1000 W/m^2, and standard spectrum, as stipulated by the definition of 'sun'.

[2]1X: flat plate collector, crystalline Si cells (0.032\$/cm^2), fixed array; 20X: nonimaging 2D Fresnel lens, concentrator cells (0.05\$/cm^2), one–axis tracking; 1000X: imaging 3D Fresnel lens, space cells (7.50\$/cm^2), full tracking.

[3]Including assembly, housing, others (Boes and Luque, 1992).

[4]Assumed to be 33% of direct cost (Zweibel and Barnett, 1992).

[5]System efficiency, including inverter, excluding lens.

[6]Flat plate with latitude tilt; one–axis, N–S tracking collector with latitude tilt; full tracking. Only direct radiation can be concentrated. Yearly average daily solar radiation for the USA; data calculated from NREL Resource Assessment Program (no year). Values for Puerto Rico; Guam (1.0/0.7/0.7); Hawaii (Honululu only: 1.0/1.0/1.0); Barstow, CA (1.0/1.0/1.2).

[7]At 1 sun: $Output = 1000\ \mathrm{W} \times \eta_{lens} \times \eta_{cell} \times \eta_{radiation}$.

Note: Current cost for c–Si system, future costs for concentrator modules for 10 MW$_p$ production volume. While 20X–systems are commercially available, 1000X–systems are not. Significant cost reductions for polycrystalline thin film (Zweibel and Barnett, 1992), or amorphous cells (Carlson and Wagner, 1992) are envisaged, reducing module cost by a factor of 8-10, while conversion efficiency will drop to around $\eta_{cell} = 0.10$. All costs are conservative estimates, based on pre–1992 data, see Boes and Luque (1992).

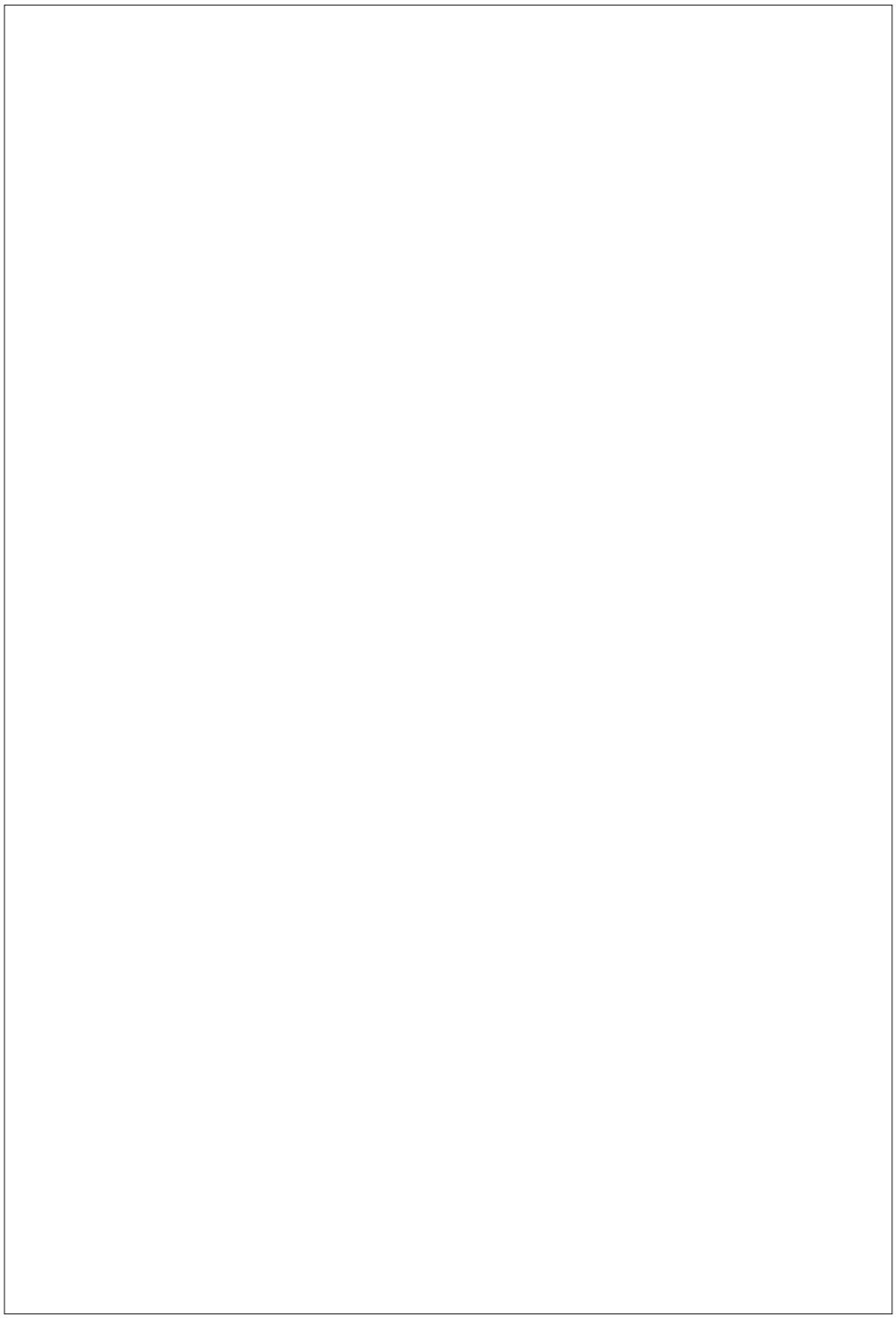

Figure 6: The first prototype of the nonimaging Fresnel lens under the sun of Tokyo, May 1999. Acceptance half angles $\theta = 2°$, $\psi = 12°$.